Pyroelectric detection of spontaneous polarization in magnetite thin films

R. Takahashi,* H. Misumi, and M. Lippmaa
Institute for Solid State Physics, University of Tokyo, 5-1-5, Kashiwanoha, Kashiwa, Chiba 277-8581, Japan
(Received 11 June 2012; revised manuscript received 3 September 2012; published 5 October 2012)

We have investigated the spontaneous polarization in Fe_3O_4 thin films by using dynamic and static pyroelectric measurements. The magnetic and dielectric behavior of Fe_3O_4 thin films grown on Nb:$SrTiO_3$(001) substrates was consistent with bulk crystals. The well-known metal-insulator (Verwey) transition was observed at 120 K. The appearance of a pyroelectric response in the Fe_3O_4 thin films just below the Verwey temperature shows that spontaneous polarization appeared in Fe_3O_4 at the charge-ordering transition temperature. The polar state characteristics are consistent with bond- and site-centered charge ordering of Fe^{2+} and Fe^{3+} ions sharing the octahedral *B* sites. The pyroelectric response in Fe_3O_4 thin films was dependent on the dielectric constant. Quasistatic pyroelectric measurement of Pd/Fe_3O_4/Nb:$SrTiO_3$ junctions showed that magnetite has a very large pyroelectric coefficient of 735 nC cm^{-2} K^{-1} at 60 K.

DOI: 10.1103/PhysRevB.86.144105 PACS number(s): 77.55.Nv, 77.55.−g, 77.55.Kt, 77.70.+a

I. INTRODUCTION

Magnetite (Fe_3O_4) is a common magnetic ferrite that has an inverse spinel structure with Fe^{3+} ions occupying the tetrahedrally coordinated *A* sites and an equal number of Fe^{2+} and Fe^{3+} ions sharing the octahedral *B* sites. Exchange interactions between the different iron sites are antiferromagnetic with the *A*-*B* sublattice exchange being dominant. This leads to ferrimagnetic spin ordering with a magnetic moment per formula unit (f.u.) close to 4.05 μ_B and a high Curie temperature of 860 K.[1–3] The magnetic properties of magnetite make it a useful material for spintronic applications, such as tunnel junctions[4,5] and spin-injection devices.[6,7] Another unique feature of Fe_3O_4 is the well-known metal-insulator Verwey transition at 120 K.[8] At room temperature, magnetite is metallic, since electrons can hop within the *B*-site lattice between the Fe^{2+} and Fe^{3+} ions. In contrast, the charges of Fe^{2+} and Fe^{3+} ions become ordered below 120 K and Fe_3O_4 crystals become insulating. A remarkable feature of the insulating Fe_3O_4 phase is the appearance of ferroelectricity. Fe_3O_4 is thus not only a prototype multiferroic material with both spontaneous magnetization and dielectric polarization, but also a rare ferroelectric crystal that appears in nature. Most other common ferroelectric crystals, such as $BaTiO_3$, Pb(Ti,Zr)O_3, etc., were artificially designed and synthesized. Studies of the ferroelectric state in Fe_3O_4 started with the magneto-electric measurements of Rado *et al.*, which indicated the presence of a polar state in Fe_3O_4 crystals at 4.2 K.[9,10] Subsequent works by Siratori *et al.* found that the magneto-electric response from Fe_3O_4 crystals was tunable by an electric field at 77 K.[11] Finally, Kato *et al.* succeeded in the observation of ferroelectric switching at 4.2 K and reported that the ferroelectric polarization along the *a* and *c* axes was 4.8 μC/cm^2 and 1.5 μC/cm^2, respectively.[12,13] Measuring ferroelectric polarization of magnetite at higher temperatures is hampered by the gradual increase of conductivity as the Verwey temperature is approached. The temperature dependence of polarization in Fe_3O_4 has therefore been studied by measuring the pyroelectric response.[14,15] Recent reports on ferroelectric Fe_3O_4 bulk crystals and thin films agree with the earlier results, showing that hysteresis loops can be measured even with a conventional ferroelectric tester, albeit only at temperatures below 40 K.[16–18]

The origin of the spontaneous polarization cannot be explained by the conventional mechanism of displacive ferroelectricity. The Fe_3O_4 low-temperature crystal structure belongs to a centrosymmetric monoclinic symmetry group (C_c),[19] which would normally preclude the existence of spontaneous polarization. However, recent theoretical work by Brink *et al.* has provided an explanation for a possible origin of ferroelectricity in Fe_3O_4.[20,21] Below the Verwey transition at 120 K, a regular arrangement of the *B*-site Fe^{2+} and Fe^{3+} ions in an inverse spinel structure results in a charge-ordered pattern. The *B* sites form a pyrochlore lattice consisting of corner-sharing tetrahedra, where an alternating pattern of Fe^{2+} and Fe^{3+} ions forms along the monoclinic *b*-axis direction of Fe_3O_4. The charge ordering results in an alternation of short and long Fe–Fe bonds. The coexistence of bond-centered and charge-centered charge ordering induces an electronic polarization along the monoclinic *b* axis.[20,22,23] This model is supported by structural analysis of powder diffraction refinements[24,25] and resonant x-ray scattering studies.[26,27] Furthermore, Senn *et al.* have recently succeeded in accurate structural analysis by high-energy x-ray diffraction from a single-domain Fe_3O_4 sample and have fully determined the low-temperature superstructure of a Fe_3O_4 crystal.[28,29] They showed that the charge ordering results in three-site distortions that induce substantial off-center atomic displacements and couple to the resulting large dielectric polarization. Similar electronic ferroelectricity induced by charge ordering is also known for $LuFe_2O_4$[30,31] and $Pr(Sr_{0.1}Ca_{0.9})_2Mn_2O_7$.[32] It is clear that in such materials there is a relationship between the pattern of charge ordering and polarization. However, there is still a discrepancy in the Fe_3O_4 experimental results, since spontaneous polarization has only been observed well below the Verwey transition point,[9–18] while x-ray and neutron diffraction studies suggest that the charge-ordered state responsible for the ferroelectricity appears at the Verwey transition and is unchanged upon further cooling.[24,26,28,29] One possible reason for this discrepancy is the high leakage current of Fe_3O_4 crystals just below the charge-ordering temperature of 120 K.

In order to investigate the relationship between the electronic polarization and the Verwey transition, we have studied by dynamic and static pyroelectric detection the temperature dependence of spontaneous polarization in Fe_3O_4 thin films grown on Nb:$SrTiO_3$(001) substrates. The pyroelectric measurement was performed at zero applied bias, which means that the results are insensitive to temperature-dependent resistivity changes close to the Verwey temperature.[33–37] The dynamic pyroelectric response of a Fe_3O_4 junction was used to study the relationship between the spontaneous polarization and the Verwey transition. Quasistatic pyroelectric analysis was used to determine the absolute pyroelectric coefficient of Pd/Fe_3O_4/Nb:$SrTiO_3$(001) junctions.

II. EXPERIMENT

The Fe_3O_4 thin films were grown by pulsed laser deposition on 0.2° miscut Nb(0.05 wt%):$SrTiO_3$(001) substrates that had been wet etched in buffered NH_4F HF to obtain a well-defined surface termination.[38,39] A polycrystalline Fe_2O_3 target was ablated with an excimer laser at a fluence of 3 J/cm^2 under an oxygen background pressure of 1×10^{-6} torr. The ablation laser (KrF, $\lambda = 248$ nm) operated at 10 Hz. The Fe_3O_4 film thicknesses were between 150 and 220 nm. The growth temperature was set at 400 °C and the temperature control was done with an infrared laser heater.[40] After growth, the films were rapidly cooled below 200 °C in about 5 min in order to suppress the oxidization of Fe and the formation of a secondary hematite Fe_2O_3 phase.[41]

The basic structural analysis was done at room temperature by symmetric x-ray diffraction and reciprocal space mapping. Magnetization of the Fe_3O_4 thin films was measured in a superconducting quantum interference device (SQUID) magnetometer at 5 and 300 K. Raman spectroscopy was used for detecting structural transitions below room temperature. A He-Ne laser (633 nm, 17 mW) was focused onto a Fe_3O_4 film surface through an objective lens (×50, N.A. = 0.5). The scattering spectra were collected by a charge-coupled device (CCD) detector (RAMASCOPE, Renishaw). The sample temperature was controlled with a He flow cryostat (Microstat, Oxford Instruments).

For electrical measurements, a 100-nm-thick Pd top electrode was deposited on the Fe_3O_4 film surface by electron beam evaporation through a stencil mask with 1 mm diameter openings. Aluminum wires were attached to the Pd top electrode pads with silver paste. The sample was placed in a vacuum chamber and cooled using a two-stage cryocooler. The sample temperature was controlled in the range of 8 to 300 K by thermal conduction from the cryocooler and a heater mounted on the sample stage. The resistance was measured by two-point method using a picoammeter (Keithley 487). The dielectric measurements were performed with an impedance bridge (Agilent 4284A) at an excitation voltage of 50 mV.

The Chynoweth method was used for dynamic pyroelectric measurements.[33–37] Chopped light from a diode laser (1.31 μm, 130 mW) was focused on a Pd top electrode pad, resulting in a modulation of the Fe_3O_4 capacitor temperature and the generation of a pyroelectric current. The laser chopping was achieved by modulating the diode laser current with an optical power risetime of ≈3 μs. The sample current was converted to a voltage signal with a current-voltage converter at a transconductance of 10^8 V/A and measured with a digital voltmeter or a lock-in amplifier. For ferroelectric hysteresis measurements, a 20-nm-thick TiN bottom electrode was inserted between a Fe_3O_4 film and a $SrTiO_3$(001) substrate in order to promote charge screening during ferroelectric switching. Details of the hysteresis loop measurements can be found in Refs. 36 and 37. A quasistatic pyroelectric measurement was used for measuring the absolute pyroelectric coefficient by slowly heating and cooling a sample in a temperature-stabilized probing chamber.[35] The pyroelectric current was measured with a picoammeter for Fe_3O_4 samples alternately heated and cooled at a constant rate, ranging from 1 to 6 K/min. The temperature of the film was monitored with a Si diode mounted next to a Fe_3O_4 capacitor sample.

III. RESULTS AND DISCUSSION

Figure 1(a) shows a reciprocal-space map around the Nb:$SrTiO_3$(103) reflection, indicating cube-on-cube growth of a (001)-oriented Fe_3O_4 film on the Nb:$SrTiO_3$(001) substrate. The in-plane and out-of-plane lattice parameters were 8.33 and 8.44 Å, consistent with the bulk lattice parameter of $a = 8.396$ Å.[42] As expected, the 150-nm-thick Fe_3O_4 film was almost fully relaxed on the $SrTiO_3$(001) substrate, since the lattice mismatch between Fe_3O_4 and $SrTiO_3$ is −7.5%.[42,43]

In general, Fe_3O_4 films are known to include antiphase boundaries (APBs) caused by random nucleation at the initial growth stage of a spinel on a perovskite substrate. The presence of such boundaries can influence the film characteristics. For example, the magnetization of defect-rich films remains unsaturated even in magnetic fields of 7 T.[44] The magnetization loops of the Fe_3O_4 thin films used in this work are shown in Fig. 1(b). The saturated magnetization was approximately 4 μ_B/f.u., matching the bulk crystal value.[1,2] The high-field data, plotted in the inset of Fig. 1(b), shows that the

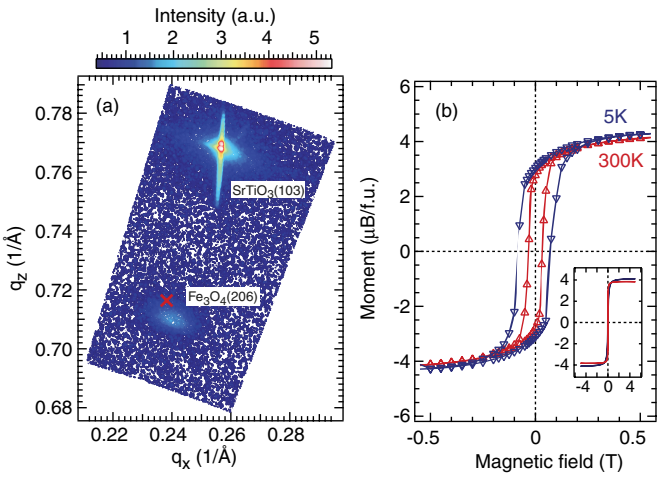

FIG. 1. (Color online) (a) Reciprocal space map of a magnetite film around the Nb:$SrTiO_3$(103) substrate reflection. The lattice parameter of bulk Fe_3O_4 crystal is marked with a cross. (b) Magnetization curves at 5 (▽: Blue) and 300 K (△: Red) for Fe_3O_4 thin films. The saturated magnetization was 4 μ_B/f.u., consistent with the bulk Fe_3O_4 magnetization. Wide-range magnetization curves measured at 5 K (Blue) and 300 K (Red) are show in the inset.

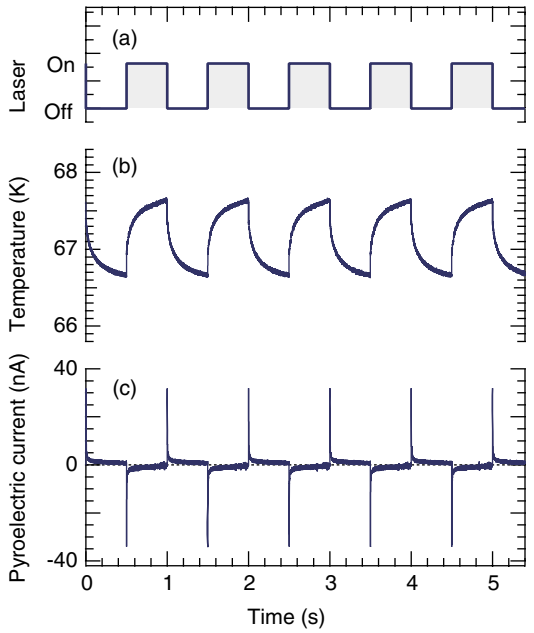

FIG. 2. (Color online) Transient profiles of the heating laser power (a), thin film sample temperature (b), and the pyroelectric current (c) for a Pd/Fe_3O_4/Nb:$SrTiO_3$ junction.

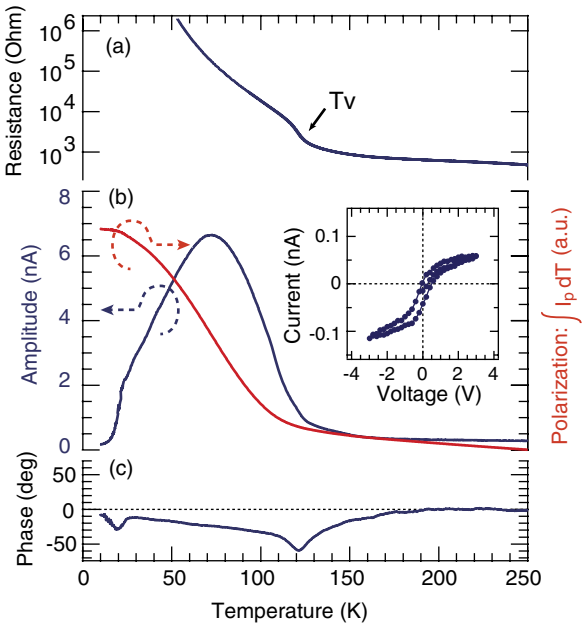

FIG. 3. (Color online) Temperature dependence of resistance (a), dynamic pyroelectric current amplitude (b), and phase (c) for a Pd/Fe_3O_4/Nb:$SrTiO_3$ junction. The Verwey transition is visible at 120 K. The right axis in (b) corresponds to the integrated pyroelectric current, showing the temperature dependence of polarization in the Fe_3O_4 film. The inset in (b) shows a hysteresis loop for a Pd/Fe_3O_4/TiN junction measured at 9 K. The polarization was switchable by an applied electric field, proving that the films were ferroelectric.

magnetization was fully saturated at fields below 2 T, suggesting that the density of APBs in our laser-ablated films was sufficiently low not to influence the attainment of magnetic saturation at this film thickness.[45] Furthermore, the temperature dependence of magnetization (not shown) showed that the Verwey transition temperature was 120 K, confirming that the Fe_3O_4 film composition was very close to stoichiometric.[46] Together with the structural analysis, the magnetic behavior showed that bulk-equivalent samples were obtained.

Figure 2 shows the transient profiles of the heating laser operation (a), sample temperature (b), and pyroelectric current (c) for a Pd/ Fe_3O_4/ Nb:$SrTiO_3$ capacitor, measured at an ambient temperature of 67 K and a laser pulse rate of 1 Hz with a 50% duty cycle. The sample temperature variation was measured with a Si diode and separately calculated from the known static temperature dependence by measuring the sample resistance variation during pulsed laser illumination. The temperature change was exponential for both heating and cooling phases of each measurement period. For a laser chopping frequency of 1 Hz, the capacitor temperature variation amplitude was estimated at 1 K, resulting in the generation of negative and positive spike currents, as shown in Fig. 2(c). The current spike is caused by the temperature dependence of the spontaneous polarization in polar materials. The measurement thus shows that spontaneous polarization existed in the Fe_3O_4 film at the measurement temperature of 67 K.

In order to investigate the relationship between the Verwey transition and the appearance of spontaneous polarization in Fe_3O_4 films, the temperature dependence of the resistance and the pyroelectric response amplitude were measured for a Pd/Fe_3O_4/Nb:$SrTiO_3$ capacitor, as shown in Fig. 3. Figure 3(a) shows the discontinuous resistance change at 120 K, corresponding to the bulk Verwey transition temperature.[8] Below the Verwey transition temperature, the pyroelectric response increased rapidly with decreasing sample temperature. As shown by the plot in Fig. 3(b), the maximum pyroelectric signal amplitude was observed at 70 K, below which the pyroelectric response was reduced. The pyroelectric current is generally proportional to the differential of the ferroelectric polarization. The temperature dependence of polarization was estimated by integrating the pyroelectric current, with the assumption that the temperature variation induced by the infrared laser was independent of the measurement temperature. The inset of Fig. 3(b) shows the hysteresis measurement result for a Pd/Fe_3O_4/TiN junction at 9 K. The pyroelectric current polarity was switched by an applied electric field, indicating the presence of ferroelectricity in the Pd/Fe_3O_4/TiN junction.

Discontinuities in the pyroelectric response can be best seen in the phase signal obtained from lock-in detection of the sample current. Figure 3(c) shows that there were two peaks at 20 and 120 K. The peak at 120 K is due to the Verwey transition and is thus related to the charge ordering of Fe^{2+} and Fe^{3+} ions. Figure 4 shows the transient profiles of laser power (a) and pyroelectric currents measured at 110 K (b), 120 K (c), and 130 K (d). At 110 and 120 K, positive and negative spike currents are clearly visible, revealing the presence of spontaneous polarization in the Fe_3O_4 thin film. In contrast, the polarization-related current spikes disappear above the Verwey transition temperature and only a contribution from the temperature-dependent leak current through the sample capacitor remains, resulting in the discontinuous modulation of pyroelectric current phase at 120 K in Fig. 3(c).

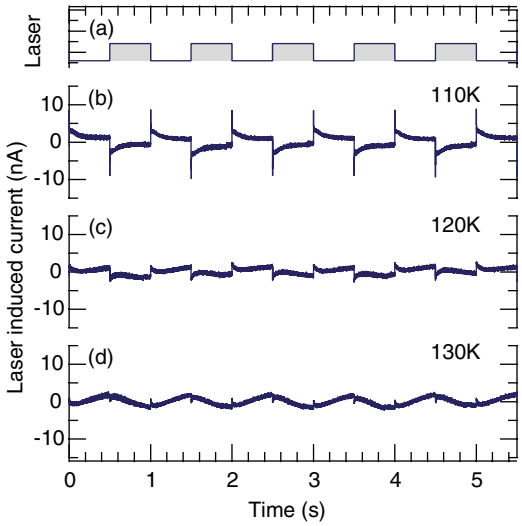

FIG. 4. (Color online) Transient profiles of the heating laser power (a) and the pyroelectric current for a Pd/Fe_3O_4/Nb:$SrTiO_3$ junction at 110 K (b), 120 K (c), and 130 K (d).

Raman measurements were performed on Fe_3O_4/Nb:$SrTiO_3$ junctions between 10 and 300 K in order to look for possible crystal symmetry changes in the thin film samples at low temperatures. The temperature dependence of the Raman spectra is shown in Fig. 5(a). A spectrum taken at 200 K, well above the Verwey temperature, is shown in Fig. 5(b). The three main features in the spectrum can be assigned to the A_{1g}, $T_{2g}(2)$, and $T_{2g}(3)$ modes by comparing the Raman shifts with literature data.[47,48] These three peaks did not show significant change between room temperature and the Verwey transition point. At the Verwey transition temperature of 120 K, the crystal structure of Fe_3O_4 changes from the high-temperature cubic phase to the low-temperature monoclinic symmetry. The effect of the symmetry reduction at the Verwey transition point can be seen

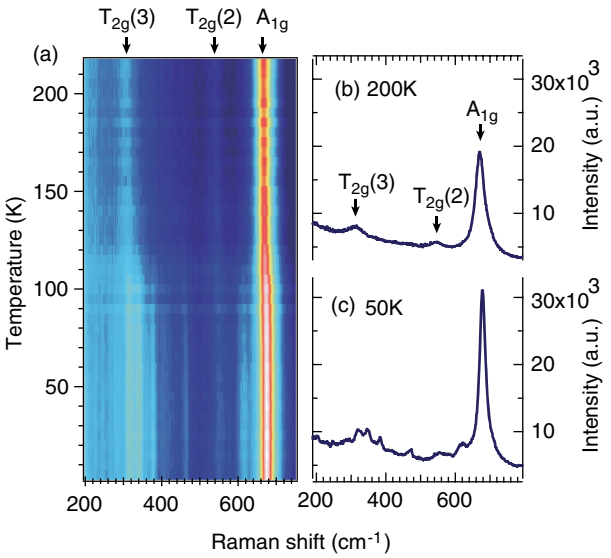

FIG. 5. (Color online) (a) Temperature dependence of Raman spectra for a Fe_3O_4 thin film. Individual Raman spectra measured at 200 K (b) and 50 K (c).

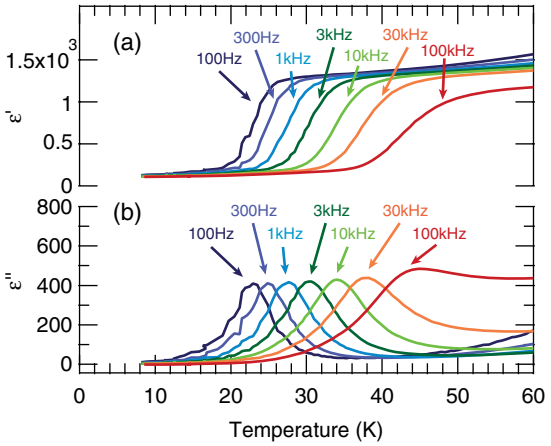

FIG. 6. (Color online) Temperature dependence of (a) dielectric permittivity ϵ' and (b) loss ϵ'' for a Pd/Fe_3O_4/Nb:$SrTiO_3$ junction for several measurement frequencies.

in the splitting of the $T_{2g}(3)$ peak into three components and a large increase in the A_{1g} peak intensity. These changes can be seen in the comparison of the 200 and 50 K Raman spectra in Figs. 5(b) and 5(c). A discontinuity in the Raman spectra occurred around 115 K, consistent with the temperature dependence of the resistance shown in Fig. 3(a). The Raman measurements reveal only a single structural transition in the 10 to 300 K temperature range, located at the Verwey temperature. No other structural changes were seen at lower temperatures. This observation is consistent with previous nuclear magnetic resonance (NMR)[49,50] and heat capacity[18] results for bulk Fe_3O_4 crystals. This implies that the peak at 20 K in Fig. 3(c) is not due to a structural transition.

The pyroelectric current amplitude is strongly dependent on the heat capacity and the thermal conductivity of a material and the sample capacitance.[34] The heat capacity of Fe_3O_4 shows a gradual monotonic decrease below the Verwey transition temperature.[18] In contrast, the thermal conductivity of Fe_3O_4 shows a gradual monotonic increase below the Verwey temperature down to about 25 K and an exponential drop at lower temperatures.[51] This suggests that the temperature variation induced by periodic heating with a chopped constant-power laser source may change at around 25 K. However, due to the small thickness of the film, the main contribution to the temperature modulation amplitude comes from the 0.5-mm-thick Nb:$SrTiO_3$ substrate. This suggests that the thermal conductivity change in Fe_3O_4 does not have a significant effect on the pyroelectric current and is not the cause for the phase jump in Fig. 3(b) around 20 K.

A clue to the origin of the phase signal feature at 20 K is offered by the measurement of the device permittivity, shown in Fig. 6, where the real and imaginary components of the magnetite film permittivity are plotted as a function of temperature for several measurement frequencies. A strong dielectric dispersion is visible, with a drop of the dielectric constant at temperatures below 50 K, consistent with previous reports.[16–18,52,53] The phase response shown in Fig. 3(c) was measured at a chopping rate of 35 Hz. At this frequency, the drop of permittivity occurs around 20 K, as shown in Fig. 6. When a pyroelectric measurement is performed at

such a dielectric transition edge, the laser-induced temperature change also modulates the device capacitance, resulting in a slight asymmetry in the heating and cooling phase pyroelectric current spikes. A lock-in current detector sees the asymmetry as a slight phase shift, explaining the phase jump at 20 K in Fig. 3(c).

The dielectric response plots in Fig. 6 show strong dispersion, which is a common feature for order-disorder type ferroelectric materials[54] and has been attributed in Fe_3O_4 to electron transfer between Fe^{2+} and Fe^{3+} ions.[52] A similar phenomenon is known to occur in the electronic ferroelectric material, $LuFe_2O_4$.[30,31] In general, the motion of a ferroelectric domain boundary gives rise to the dispersion, indicating the presence of ferroelectric domains and boundary motion. In order to investigate the dielectric dispersion in Fe_3O_4 films, the frequency dependence of ϵ' and ϵ'' were measured at 19, 25, 31, and 37 K, and plotted in Figs. 7(a) and 7(b), showing a typical signature of relaxation. A stepwise change in ϵ' is accompanied by a ϵ'' peak. At higher temperatures, the peak position of ϵ'' shifted to higher frequencies, implying that the relaxation time τ became smaller, since $\tau = 1/(2\pi \times \text{frequency})$. The

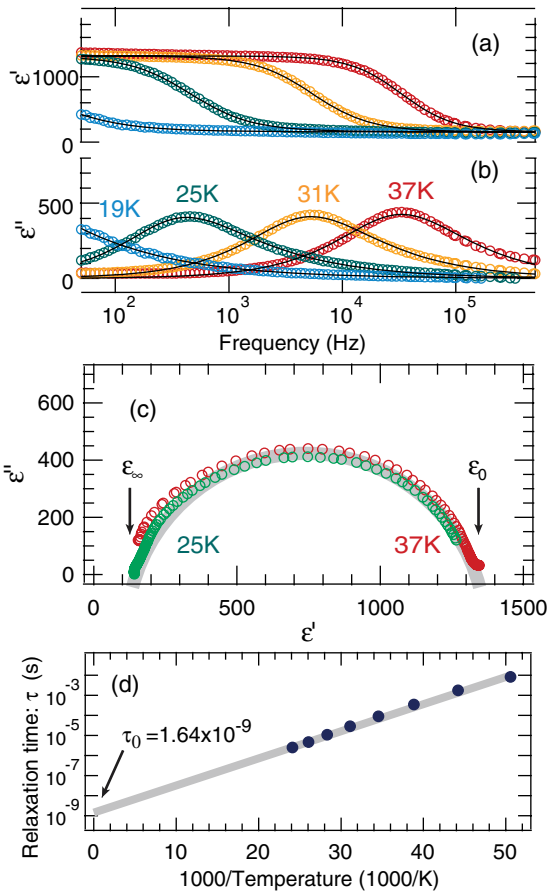

FIG. 7. (Color online) Frequency dependence of (a) ϵ' and (b) ϵ'' for a $Pd/Fe_3O_4/Nb:SrTiO_3$ junction for several measurement temperatures. The circles and solid lines represent the measured data and the Havriliak-Negami fitting results, respectively. (c) Cole-Cole plot of ϵ' and ϵ'', yielding estimates for $\epsilon_\infty = 135$ at 25 K and $\epsilon_0 = 1340$ at 37 K. (d) Arrhenius plot of relaxation times obtained from the Havriliak-Negami fitting. The activation energy and prefactor were estimated at 26.8 meV and 1.64 ns.

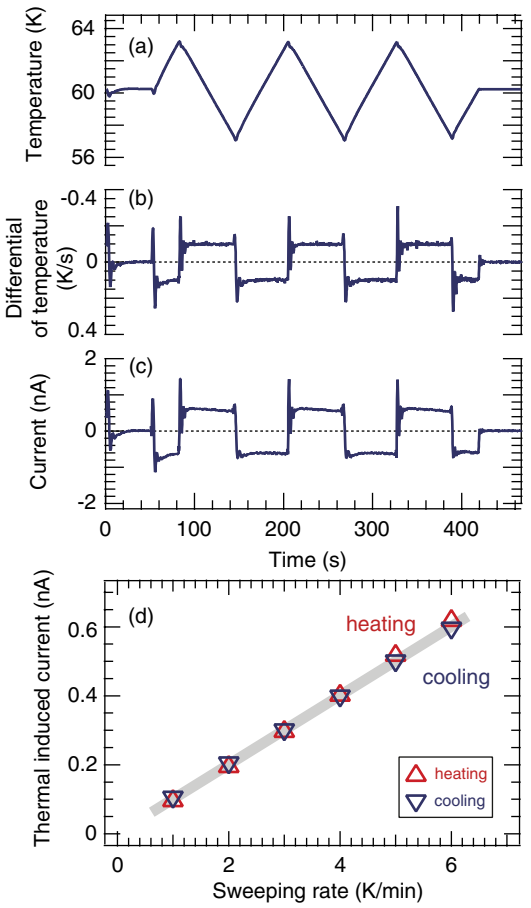

FIG. 8. (Color online) Static pyroelectric response for a $Pd/Fe_3O_4/Nb:SrTiO_3$ junction. (a) Time profile of the slow heating and cooling cycles applied to the sample. (b) Differential of temperature cycle. (c) A constant pyroelectric current was observed when the film was heated or cooled at a constant rate at an average temperature of 60 K. (d) The effective pyroelectric coefficient estimated from the slope of the thermally induced current was 735 nC cm^{-2} K^{-1}.

empirical Havriliak-Negami function[55] was used to quantitatively analyze the dielectric relaxation behavior:

$$\epsilon' - i\epsilon'' = \epsilon_\infty + \frac{\epsilon_0 - \epsilon_\infty}{[1 + (i\omega\tau)^{1-\alpha}]^\beta}, \tag{1}$$

where ϵ_∞ and ϵ_0 are the high- and low-frequency dielectric constants, respectively, and α and β represent the broadening and asymmetry factors of the curves. The permittivities estimated from the Cole-Cole plots in Fig. 7(c) were $\epsilon_\infty = 135$ and $\epsilon_0 = 1340$. After substituting the estimated ϵ_∞ and ϵ_0 into Eq. (1), α, β, and τ were optimized. The fitting results are shown by solid lines in Figs. 7(a) and 7(b). The Havriliak-Negami function provides excellent fits for the observed dielectric dispersion. Figure 7(d) shows values of τ from the fitting results in an Arrhenius representation.

$$\tau = \tau_0 \exp\left(\frac{E_a}{k_B T}\right), \tag{2}$$

where τ_0 is a prefactor, $k_B T$ is the thermal energy, and E_a is the activation energy. The observed linear slope in Fig. 7(d) shows that the dielectric relaxation is thermally activated with $E_a = 26.8$ meV, which is close to the reported values for

bulk and film Fe_3O_4.[16–18,52,53] Linear extrapolation yields a prefactor value of $\tau_0 = 1.64$ ns, corresponding to a rather low attempt frequency of less than 100 MHz. This value is much lower than the 280 GHz of a typical electronic ferroelectric, $LuFe_2O_4$,[30] and would appear to show that much larger effective domain sizes are involved.[28,29]

The large dielectric constant above 50 K plays an important role in Pd/Fe_3O_4/Nb:$SrTiO_3$ junctions for obtaining the strong pyroelectric response shown in Figs. 2 and 3(b). The maximum pyroelectric current in Fig. 3(b) is approximately 7 nA and independent of the polarity of the poling bias. In order to evaluate the absolute value of the pyroelectric coefficient, a quasistatic pyroelectric measurement without the use of laser illumination was performed for a Pd/Fe_3O_4/Nb:$SrTiO_3$ junction at 60 K. This method can be used to eliminate possible photoinduced currents that may affect the dynamic pyroelectric measurements.[37] Figures 8(a)–8(c) show the slow sample temperature sweep, the measured sample temperature gradient, and the observed pyroelectric current, respectively. The temperature sweep rate was 6 K/min. At a constant average temperature of 60 K, there was no generated current, as expected for dark conditions. During the heating slope, a constant negative pyroelectric current was generated and a corresponding positive pyroelectric current was observed for the cooling slope. This can be verified by comparing Figs. 8(b) and 8(c). The transient spikes in the differential of the sample temperature in Fig. 8(b) are caused by the finite settling time of the temperature controller and corresponding pyroelectric current spikes can also be seen in Fig. 8(c). The nonideal temperature controller performance thus served as a convenient way to check that the observed slow pyroelectric response is consistent with the faster response measured in the dynamic measurements with chopped optical heating.

The static pyroelectric current was proportional to the temperature sweep rate, as shown in Fig. 8(d). From the slope of a linear fit of the data points, the effective pyroelectric coefficient at 60 K was estimated to be 735 nC cm^{-2} K^{-1}. This value is comparable to the well-known large pyroelectric coefficient of Pb(Sc,Ta)O_3 films, 600 nC cm^{-2} K^{-1},[56] and much larger than, for example, in $PbTiO_3$/MgO films, 20 nC cm^{-2} K^{-1}.[57] We note that the pyroelectric coefficient involves a piezoelectric contribution due to a difference in the thermal expansion coefficients of the Fe_3O_4 film and the Nb:$SrTiO_3$ substrate.[34,35]

IV. CONCLUSION

We have demonstrated dynamic and static pyroelectric measurements of Fe_3O_4 thin film capacitors. It was shown that the polar state in Fe_3O_4 does indeed appear at the Verwey transition point. The relaxor behavior at low temperatures is consistent with the spontaneous polarization being induced by bond- and site-centered charge ordering of Fe^{2+} and Fe^{3+} ions sharing the octahedral *B* sites.

The dynamic pyroelectric response was influenced by the sharp change of the dielectric permittivity in the 20 to 50 K range. The dielectric transition at ≈20 K was confirmed not to be caused by a structural transition. The slow characteristic time scale of the relaxor response at ≈1 ns appears to indicate that the charge-ordered relaxor domains involve a large number of iron sites. Static pyroelectric measurement were used to show that magnetite has a very large pyroelectric coefficient of 735 nC cm^{-2} K^{-1} at 60 K.

ACKNOWLEDGMENTS

The authors would like to thank the Asahi Glass Foundation, the Futaba Electronics Memorial Foundation, the Foundation for Interaction in Science & Technology, and the Murata Science Foundation for funding.

*rtaka@issp.u-tokyo.ac.jp

[1] F. Walz, J. Phys.: Condens. Matter **14**, 285R (2002).
[2] M. Opel, J. Phys. D: Appl. Phys. **45**, 033001 (2012).
[3] M. Monti, B. Santos, A. Mascaraque, O. R. de la Fuente, M. A. Nino, T. O. Mentes, A. Locatelli, K. F. MacCarty, J. F. Marco, and J. de la Figuera, Phys. Rev. B **85**, 020404 (2012).
[4] P. Seneor, A. Fert, J. L. Maurice, F. Montaigne, F. Petroff, and A. Vaures, Appl. Phys. Lett. **74**, 4017 (1999).
[5] P. J. van der Zaag, P. J. H. Bloemen, J. M. Gaines, R. M. Wolf, P. A. A. van der Heijden, R. J. M. van de Veerdonk, and W. J. M. de Jonge, J. Magn. Magn. Mater. **211**, 301 (2000).
[6] E. Wada, K. Watanabe, Y. Shirahata, M. Itoh, M. Yamaguchi, and T. Taniyama, Appl. Phys. Lett. **96**, 102510 (2010).
[7] S. Yamanaka, T. Kanki, T. Kawai, and H. Tanaka, Nano Lett. **11**, 343 (2011).
[8] E. J. W. Verwey, Nature (London) **144**, 327 (1939).
[9] G. T. Rado and J. M. Ferrari, Phys. Rev. B **12**, 5166 (1975).
[10] G. T. Rado and J. M. Ferrari, Phys. Rev. B **15**, 290 (1977).
[11] K. Siratori, E. Kita, G. Kaji, A. Tasaki, S. Kimura, I. Shindo, and K. Kohn, J. Phys. Soc. Jpn. **47**, 1779 (1979).
[12] K. Kato and S. Iida, J. Phys. Soc. Jpn. **51**, 1335 (1982).
[13] K. Kato, S. Iida, K. Yanai, and K. Mizushima, J. Magn. Magn. Mater. **31–34**, 783 (1983).
[14] Y. Miyamoto, M. Kobayashi, and S. Chikazumi, J. Phys. Soc. Jpn. **55**, 660 (1986).
[15] T. Inase and Y. Miyamoto, J. Phys. Soc. Jpn. **56**, 3683 (1987).
[16] M. Alexe, M. Ziese, D. Hesse, P. Esquinazi, K. Yamauchi, T. Fukushima, S. Picozzi, and U. Gosele, Adv. Mater. **21**, 4452 (2009).
[17] M. Ziese, P. D. Esquinazi, D. Pantel, M. Alexe, N. M. Nemes, and M. Gercia-Hernandez, J. Phys.: Condens. Matter **24**, 086007 (2012).
[18] F. Schrettle, S. Krohns, P. Lunkenheimer, V. A. M. Brabers, and A. Loidl, Phys. Rev. B **83**, 195109 (2011).
[19] M. Iizumi, T. F. Koetzle, G. Shirane, S. Chikazumi, M. Matsui, and S. Todo, Acta Crystallogr., Sect. B: Struct. Crystallogr. Cryst. Chem. **38**, 2121 (1982).
[20] J. Brink and D. I. Khomskii, J. Phys.: Condens. Matter **20**, 424217 (2008).

[21]D. V. Efremov, J. V. D. Brink, and D. I. Khomskii, Nat. Mater. **3**, 853 (2004).
[22]K. Yamauchi, T. Fukushima, and S. Picozzi, Phys. Rev. B **79**, 212404 (2009).
[23]T. Fukushima, K. Yamauchi, and S. Picozzi, J. Phys. Soc. Jpn. **80**, 014709 (2011).
[24]J. P. Wright, J. P. Attfield, and P. G. Radaelli, Phys. Rev. Lett. **87**, 266401 (2001).
[25]J. Blasco, J. Garcia, and G. Subias, Phys. Rev. B **83**, 104105 (2011).
[26]Y. Joly, J. E. Lorenzo, E. Nazarenko, J. L. Hodeau, D. Mannix, and C. Marin, Phys. Rev. B **78**, 134110 (2008).
[27]J. E. Lorenzo, C. Mazzoli, N. Jaouen, C. Detlefs, D. Mannix, S. Grenier, Y. Joly, and C. Marin, Phys. Rev. Lett. **101**, 226401 (2008).
[28]M. S. Senn, J. P. Wright, and P. A. Attfield, Nature (London) **481**, 173 (2012).
[29]M. S. Senn, I. Loa, J. P. Wright, and J. P. Attfield, Phys. Rev. B **85**, 125119 (2012).
[30]N. Ikeda, H. Ohsumi, K. Ohwada, K. Ishii, T. Inami, K. Kakurai, Y. Murakami, K. Yoshii, S. Mori, Y. Horibe, and H. Kito, Nature (London) **436**, 1136 (2005).
[31]N. Ikeda, K. Kohn, N. Myouga, E. Takahashi, H. Kitoh, and S. Takekawa, J. Phys. Soc. Jpn. **69**, 1526 (2000).
[32]Y. Tokunaga, T. Lottermoser, Y. Lee, R. Kumai, M. Uchida, T. Arima, and Y. Tokura, Nat. Mater. **5**, 937 (2006).
[33]A. G. Chynoweth, J. Appl. Phys. **27**, 78 (1956).
[34]M. E. Lines and A. M. Glass, *Principles and Applications of Ferroelectrics and Related Materials* (Oxford University Press, New York, 1977).
[35]A. V. Bune, C. Zhu, S. Ducharme, L. M. Blinov, V. M. Fridkin, S. P. Palto, N. G. Petukhova, and S. G. Yudin, J. Appl. Phys. **85**, 7869 (1999).
[36]R. Takahashi, M. Katayama, O. Dahl, J. K. Grepstad, Y. Matsumoto, and T. Tybell, Appl. Phys. Lett. **94**, 232901 (2009).
[37]R. Takahashi, T. Tybell, and M. Lippmaa, J. Appl. Phys. **112**, 014111 (2012).
[38]M. Kawasaki, K. Takahashi, T. Maeda, R. Tsuchiya, M. Shinohara, O. Ishiyama, T. Yonezawa, M. Yoshimoto, and H. Koinuma, Science **266**, 1540 (1994).
[39]G. Koster, B. L. Kropman, G. J. H. M. Rijnders, D. H. A. Blank, and H. Rogalla, Appl. Phys. Lett. **73**, 2920 (1998).
[40]S. Ohashi, M. Lippmaa, N. Nakagawa, H. Nagasawa, H. Koinuma, and M. Kawasaki, Rev. Sci. Instrum. **70**, 178 (1999).
[41]R. Takahashi, H. Misumi, and M. Lippmaa, Cryst. Growth Des. **12**, 2679 (2012).
[42]JCPDS Card 19-0629.
[43]JCPDS Card 35-0734.
[44]D. T. Margulies, F. T. Parker, F. E. Spada, R. S. Goldman, J. Li, R. Sinclair, and A. E. Berkowitz, Phys. Rev. B **53**, 9175 (1996).
[45]T. Hibma, F. C. Voogt, L. Niesen, P. A. A. van der Heijden, and W. J. M. de Jonge, J. Appl. Phys. **85**, 5291 (1999).
[46]R. Aragon, D. J. Buttrey, J. P. Shepherd, and J. M. Honig, Phys. Rev. B **31**, 430 (1985).
[47]J. L. Verble, Phys. Rev. B **9**, 5236 (1974).
[48]D. M. Phase, S. Tiwari, R. Prakash, A. Dubey, V. G. Sathe, and R. J. Choudhary, J. Appl. Phys. **100**, 123703 (2006).
[49]N. M. Kovtun and A. A. Shamyakov, Solid State Commun. **13**, 1345 (1973).
[50]K. Yanai, M. Mizoguchi, and S. Iida, J. Phys. Soc. Jpn **50**, 65 (1981).
[51]G. A. Slack, Phys. Rev. **126**, 427 (1962).
[52]K. Iwauchi, Y. Kita, and N. Koizumi, J. Phys. Soc. Jpn. **49**, 1328 (1980).
[53]M. Kobayashi, Y. Akishige, and E. Sawaguchi, J. Phys. Soc. Jpn. **57**, 3474 (1988).
[54]D. Fu, H. Taniguchi, M. Itoh, S. Y. Koshihara, N. Yamamoto, and S. Mori, Phys. Rev. Lett. **103**, 207601 (2009).
[55]S. Havriliak and S. Negami, Polymer **8**, 161 (1967).
[56]R. Watton and M. A. Todd, Ferroelectrics **118**, 279 (1991).
[57]K. Iijima, Y. Tomita, R. Takayama, and I. Ueno, J. Appl. Phys. **60**, 361 (1986).